Optimality and Noise Resilience of Critical Quantum Sensing

U. Alushi,[1,2,*] W. Górecki,[3,*] S. Felicetti,[2,4,†] and R. Di Candia[1,5,‡]
[1]Department of Information and Communications Engineering, Aalto University, Espoo 02150, Finland
[2]Institute for Complex Systems, National Research Council (ISC-CNR), Via dei Taurini 19, 00185 Rome, Italy
[3]INFN Sez. Pavia, via Bassi 6, I-27100 Pavia, Italy
[4]Physics Department, Sapienza University, P.le A. Moro 2, 00185 Rome, Italy
[5]Dipartimento di Fisica, Università degli Studi di Pavia, Via Agostino Bassi 6, I-27100 Pavia, Italy

(Received 29 February 2024; accepted 10 June 2024; published 22 July 2024)

We compare critical quantum sensing to passive quantum strategies to perform frequency estimation, in the case of single-mode quadratic Hamiltonians. We show that, while in the unitary case both strategies achieve precision scaling quadratic with the number of photons, in the presence of dissipation this is true only for critical strategies. We also establish that working at the exceptional point or beyond threshold provides suboptimal performance. This critical enhancement is due to the emergence of a transient regime in the open critical dynamics, and is invariant to temperature changes. When considering both time and system size as resources, for both strategies the precision scales linearly with the product of the total time and the number of photons, in accordance with fundamental bounds. However, we show that critical protocols outperform optimal passive strategies if preparation and measurement times are not negligible. Our results are applicable to a broad variety of critical sensors whose phenomenology can be reduced to that of a single-mode quadratic Hamiltonian, including systems described by finite-component and fully connected models.

DOI: 10.1103/PhysRevLett.133.040801

Introduction—The susceptibility developed in proximity of critical phase transitions (PTs) is a valuable resource in metrological tasks. This concept is widely exploited in advanced sensors such as transition-edge detectors and bubble chambers. However, these devices make use of a classical sensing strategy, and they are not optimal from a quantum-metrology perspective [1,2]. The recently introduced research field of critical quantum sensing (CQS) consists of leveraging quantum PTs to design quantum-enhanced sensors [3–14]. In the last few years, it has been theoretically shown that it is possible to achieve quantum advantage in sensing exploiting both static [3–11] and dynamical [12–14] critical properties of many-body quantum systems. The first experimental demonstrations of quantum-enhanced sensing have been achieved with Rydberg atoms [15] and nuclear magnetic resonance techniques [16].

Quantum advantage in sensing is defined in terms of the scaling of achievable precision with respect to fundamental resources, such as system size and protocol duration time. Despite the critical slowing down, it has been shown [17] that CQS protocols implemented on many-body spin systems can achieve Heisenberg scaling [18] in both time and system size. This result has been recently extended [19] to the class of finite-component PTs, which can take place in quantum resonators with atomic [20–24] or Kerr [25–28] nonlinearities. In contrast to many-body spin systems, where criticality emerges in the limit of an infinite number

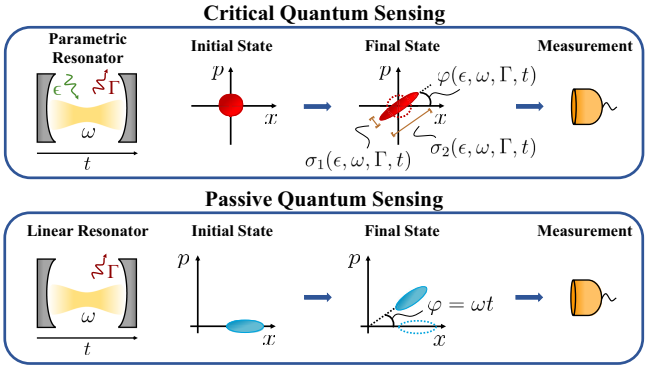

FIG. 1. Sketch of CQS and PQS strategies. Top: in CQS, the system, initially at the equilibrium with the environment, evolves according to (1). The final state is a squeezed thermal state with covariance matrix depending nontrivially on the system parameters. An optimal measurement is homodyne with an optimized angle, regardless of the system parameters. Bottom: the initial state of PQS, an optimized displaced squeezed thermal state, acquires a phase shift $\varphi = \omega t$ in the free time evolution. Here, to saturate the QFI, a nonlinear measurement is needed in some parameter regimes. In both strategies, we consider interaction with a thermal environment as in (2).

*These authors contributed equally to this letter.
†Contact author: felicetti.simone@gmail.com
‡Contact author: rob.dicandia@gmail.com

of atoms, in finite-component models this thermodynamic limit is replaced with a rescaling of the physical parameters. While many-body spin systems become critical in the thermodynamic limit (infinite number of atoms), finite-component PTs are formally defined by a parameter-rescaling limit [21,26] applied to a nonlinear bosonic system (infinite number of photons).

On the one hand, finite-component PTs make it possible to implement CQS protocols with small-scale devices, such as parametric resonators [29–32], single trapped ions [33], optomechanical [34,35] or magnomechanical [36] devices, spin impurities [37], and Rabi-like systems [38–40]. On the other hand, finite-component PTs, as well as fully connected systems [41–43], can be effectively described with minimal models, and so they provide a compelling theoretical framework to analyze CQS protocols with analytical or semianalytical methods [19,30,41,44–49]. Recent theoretical efforts have been dedicated to the identification and design of optimal CQS protocols. It has been shown that the dynamical approach has a constant-factor advantage over static protocols [41,45]. An apparent super-Heisenberg scaling can be achieved when focusing on a specific resource such as system size [46,47] or time [48]. CQS protocols achieve quantum advantage also for global sensing using adaptive strategies [50,51] in the driven-dissipative case with continuous measurements [52,53] and in the multiparameter case [8,37,54]. Beyond the analysis of specific applicable protocols, in recent years, fundamental bounds on the quantum Fisher information (QFI) [1] have been derived [55–59]. Not only do they allow quick identification of which systems can benefit from quantum metrology, but they also clarify what should be considered a resource in metrology.

In this Letter, we fill several knowledge gaps in the understanding of criticality-enhanced protocols, by putting them in a general quantum metrology framework. We compare the performances of CQS and the standard quantum metrology approach, i.e., passive quantum sensing (PQS), in the frequency estimation task. We first consider only the system size as a resource. In the noiseless case, we find that, despite both strategies achieving Heisenberg scaling, optimal PQS outperforms CQS protocols by a constant factor. However, in the more realistic case of parameter estimation in dissipative dynamics, only CQS shows a *quadratic* scaling of the single-shot QFI in the number of photons. This critical enhancement appears with the emergence of a transient regime from the unitary to the steady-state dynamics, where the QFI grows. Such a regime can be arbitrarily long, and is not present in the absence of dissipation. Then, we consider both time and system size as resources, and we frame our results within the context of ultimate precision bounds. Here, there is a critical enhancement if preparation and/or measurement times are non-negligible. Finally, we show that our results stand also in the presence of thermal noise.

Throughout the Letter, we heavily use Gaussian quantum information methods for the solution of dynamics and for the computation of quantum and classical Fisher information [60–62]. To provide meaningful discussion, we may use approximations in the relevant regimes. However, all calculations are analytical, and their details are in the Supplemental Material [63]. See Sec. I of the Supplemental Material for a summary of the tools used.

Critical quantum sensing—We consider an idealized setting where the phenomenology of interest for CQS is described by the squeezing Hamiltonian,

$$H = \omega a^\dagger a + \frac{\epsilon}{2}(a^2 + a^{\dagger 2}), \tag{1}$$

where ϵ is the squeezing parameter and $\omega = \omega_0 + \delta\omega$ is the sum of a known frequency ω_0 and an unknown, small, frequency shift $\delta\omega$ to be estimated. This minimal model can effectively describe [41] the low-energy physics of a broad variety of criticalities emerging in (i) finite-component systems such as the quantum Rabi model [21,64], driven Kerr resonators [25,65,66], ultrastrongly coupled resonators [26] and (ii) fully connected models, such as the Dicke [42] and the Lipkin-Meshkov-Glick [43]. This system can be thought of as a Kerr resonator in the Gaussian approximation, i.e., in the limit of small Kerr nonlinearity. In this limit, the system undergoes a second-order phase transition at the critical value $\epsilon = \epsilon_c = \sqrt{\omega^2 + \Gamma^2}$ [30]. The effect of higher-order nonlinearities can be neglected until the photon number is sufficiently small; see the Supplemental Material [63], Sec. II. The limits of validity of the approximation will be specific to each platform, and are not within the scope of this work. We assume that the parameters ω_0 and ϵ can be independently tuned, while $\delta\omega$ depends on some external field to be probed. To provide a practical example, the most direct implementation consists of a superconducting quantum resonator [65–68], where ϵ corresponds to the intensity of an external parametric drive, ω_0 is the detuning of the bare resonance frequency with respect to half the pump frequency, while $\delta\omega$ is directly proportional to an external magnetic flux. We consider a coupling to a thermal bath, described by the Lindbladian

$$\begin{aligned}\mathcal{L}[\cdot] = {} & \Gamma(1+n_B)\left(2a\cdot a^\dagger - \{a^\dagger a, \cdot\}\right) \\ & + \Gamma n_B\left(2a^\dagger \cdot a - \{aa^\dagger, \cdot\}\right),\end{aligned} \tag{2}$$

where $\Gamma \geq 0$ is the environment-system coupling strength and n_B is the effective temperature of the bath.

We analyze a CQS protocol consisting of estimating the parameter $\delta\omega$ by choosing properly optimized values of ω_0 and ϵ; see Fig. 1. Without loss of generality, we consider a constraint on the maximum average number of photons in the resonator, call it $N_{\max}$, that can theoretically be set arbitrarily large. This constraint is physically motivated as the model (1) is the result of different approximations working for finite $N_{\max}$, such as the dispersive approximation when the

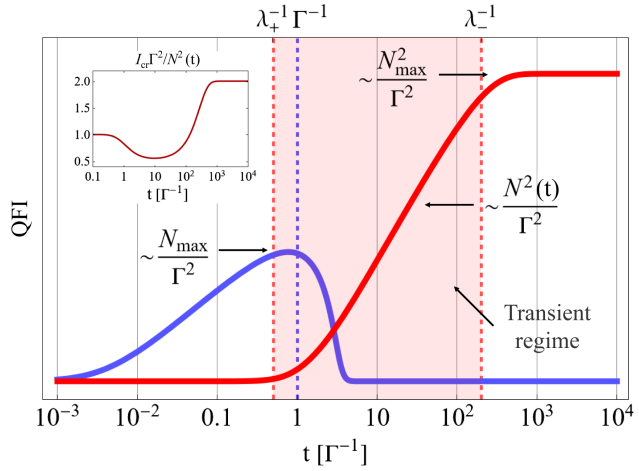

FIG. 2. Single-shot QFI. Comparison of the single-shot QFI between PQS (blue) and CQS (red), at zero temperature, for $\omega_0 = \Gamma$ and $N_{\max} = 100$. The vertical axis has been rescaled as $\log(1 + \mathrm{QFI})$ for better visibility. For PQS, the optimal measurement time is $t \simeq 0.8/\Gamma$. For CQS, the optimal ϵ is $\epsilon_{\mathrm{opt}} = \sqrt{[2N_{\max}/(1+2N_{\max})]}\epsilon_c$. The critical enhancement is due to the emergence of the transient regime in the dissipative case, where the QFI grows with quadratic scaling with N until reaching the steady state; see inset.

resonator is coupled to an off resonance qubit, or the Gaussian approximation [30,41].

Passive quantum sensing—PQS for the frequency estimation problem consists of initializing a linear resonator to a quantum state ρ, and letting it evolve according to the free Hamiltonian $H_0 = \omega a^\dagger a$ under the influence of noise in (2); see Fig. 1. As in CQS, we assume that $\omega = \omega_0 + \delta\omega$, where $\delta\omega$ is to be estimated. PQS assumes no active control over the resonator during the evolution, aside from choosing the interaction time. We consider the initial state generated with a generic unitary Gaussian operation applied to the state at the equilibrium with the environment, i.e., $\rho = D(\alpha)S(r)\rho_B S^\dagger(r)D^\dagger(\alpha)$, where ρ_B is a thermal state with n_B photons, $D(\alpha)$ and $S(r)$ are displacement and squeezing operations respectively, and the total number of photons is constrained to $N_{\max} = |\alpha|^2 + (1+2n_B)\sinh^2(r) + n_B$.

The noiseless case ($\Gamma = 0$, $n_B = 0$)—Here, the QFI for estimating $\delta\omega$ with CQS is $I_{\mathrm{cr}} \sim [2N(t) + 8N^2(t)/9]t^2$ for $\epsilon \to \epsilon_c$, where $N(t) \sim \omega_0^2 t^2$. Details of the derivation can be found in the Supplemental Material [63], Sec. III, where it is also shown that homodyne measurements saturate the QFI. Notice that, with constraints on both $N_{\max}$ and the total time T, the optimal choice is to set $\omega_0 = \sqrt{N_{\max}}/T$, so we can use all resources coherently. For PQS, by optimizing over Gaussian input states with $N_{\max}$ number of photons, we get $I_{\mathrm{pas}} = 8N_{\max}(1+N_{\max})t^2$. The optimal value is given by a squeezed-vacuum state; see the Supplemental Material [63], Sec. IV. Assuming $N(t) \leq N_{\max}$, I_{pas} is always larger than I_{cr} by a constant factor. This comes with no surprise, as PQS protocol is initialized with $N_{\max}$ photons while CQS is initialized with the vacuum. Here, the main message is that both protocols show quantum advantage, achieving the Heisenberg scaling $\propto (N_{\max}T)^2$. Notice that this analysis holds also for $\Gamma > 0$, as long as $t \ll (N_{\max}\Gamma)^{-1}$.

What part of this quantum advantage will survive for longer times, where the effects of noise become significant? In the following, we first discuss the scaling of the *single-shot* QFI with $N_{\max}$, therefore momentarily neglecting time as a resource. This will turn out to be useful for understanding the scaling of QFI with *both* T and $N_{\max}$, which will be then related to ultimate precision bounds.

Zero-temperature dissipative case ($\Gamma > 0$, $n_B = 0$)—In the dissipative scenario, we recognize two different timescales for the critical dynamics, defined by the real parts of the Liouvillian eigenvalues $\lambda_\pm = \Gamma \pm \sqrt{\epsilon^2 - \omega^2}$. Here, $\mathrm{Re}(\lambda_+)^{-1}$ is the timescale when the dynamic stops being effectively unitary, while $\mathrm{Re}(\lambda_-)^{-1}$ is the timescale to reach the steady state. For $\epsilon \leq \omega$ these times are equal, while for $\epsilon > \omega$ both $\lambda_\pm$ are real and different. This results in the emergence of a transient regime; see Fig. 2. Approaching the critical point $\epsilon \to \epsilon_c$ makes the steady-state time diverge since $\lambda_-^{-1} \sim \Gamma/\epsilon_c(\epsilon_c - \epsilon)$, so the transient regime can be arbitrarily long.

Let us switch to the problem of estimating $\delta\omega$. We consider $\epsilon > \omega_0$, and we work at $\omega_0 = \Gamma$, which maximizes the QFI; see the Supplemental Material [63], Sec. III. Also in the dissipative case, the optimal measurement is homodyne. From Fig. 2, we see that the interesting part is the transient regime, where the QFI is $I_{\mathrm{cr}} \gtrsim N^2(t)/2\Gamma^2$. The maximal QFI to N^2 rate is achieved at the steady state, where $I_{\mathrm{cr}} \simeq 2N^2(\infty)/\Gamma^2$; see the inset of Fig. 2. The mean number of photons $N(t)$ increases monotonically in time and saturates at $N(\infty) = \epsilon^2/2(\epsilon_c^2 - \epsilon^2)$. Looking for an optimal strategy with constraints on $N_{\max}$, since the optimal rate is at the steady state, the optimal choice of ϵ will be the one for which $N(\infty) = N_{\max}$, i.e., $\epsilon_{\mathrm{opt}} = \sqrt{[2N_{\max}/(1+2N_{\max})]}\epsilon_c$. This analysis also shows that working close to the exceptional point $\epsilon \simeq \omega_0$ is a suboptimal choice, as at this point the number of photons is severely bounded.

For PQS, the QFI for estimating $\delta\omega$ is [69]

$$I_{\mathrm{pas}} = \left[\frac{4\alpha^2}{e^{-2r} + e^{2\Gamma t} - 1} + \frac{e^{-2r}(e^{4r}-1)^2}{2e^{2r+4\Gamma t} + (e^{2r}-1)^2(e^{2\Gamma t}-1)}\right] t^2. \tag{3}$$

Let us consider $t \gtrsim (N_{\max}\Gamma)^{-1}$. Under the condition $e^{2r} \gg e^{4\Gamma t}/(e^{2\Gamma t} - 1)$, we get the simple expression

$$I_{\mathrm{pas}} \simeq \frac{4N_{\max}t^2}{e^{2\Gamma t} - 1}. \tag{4}$$

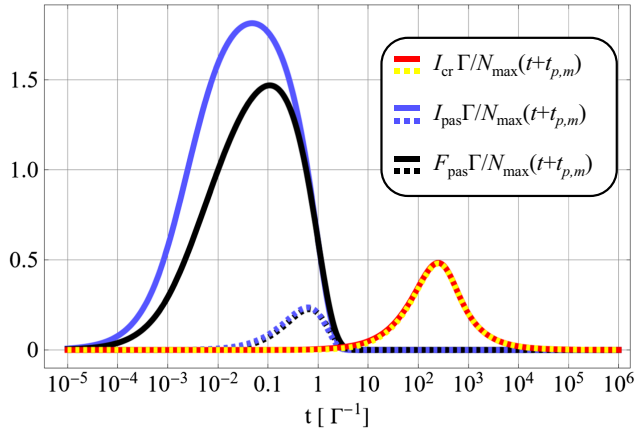

FIG. 3. QFI rate. Comparison of the ratios $I_{\mathrm{pas,cr}}/N_{\max}(t+t_{p,m})$ for the PQS (blue) and CQS (red), at zero temperature, for $t_{p,m}=0$ (solid lines) and $t_{p,m}=2/\Gamma$ (dashed lines). In black, we draw the same type of plot for the Fisher information of homodyne measurement in PQS. Here, we set $N_{\max}=100$, $\epsilon=\epsilon_{\mathrm{opt}}$, $\omega_0=\Gamma$. By neglecting preparation and measurement time, the passive strategy is fundamentally optimal for large enough $N_{\max}$, as it saturates the ultimate precision bounds. Even for finite $N_{\max}$, it performs significantly better than the critical strategy. However, by considering $t_{p,m}>0$, while the QFI rate is significantly reduced for PQS, it remains essentially unchanged for CQS. In this framework, there is a critical enhancement.

The condition on r can be easily satisfied also at finite $N_{\max}$ if Γt is not too large. One can see that, to optimize the QFI, the exact amount of squeezing is not crucial as long as it guarantees the condition on r. The QFI (4) is optimal for $t\simeq 0.8/\Gamma$, for which $I_{\mathrm{pas}}=O(N_{\max}/\Gamma^2)$; see Fig. 2. We should notice that the first term in (3) corresponds to the Fisher information for homodyne measurement of the p quadrature, which saturates the QFI for $t\gtrsim(N_{\max}\Gamma)^{-1}$ already when $N_{\max}\gtrsim 10^3$; see the Supplemental Material [63], Sec. IV.

We see a difference in scaling in the number of photons between CQS and PQS as $I_{\mathrm{cr}}=O(N_{\max}^2/\Gamma^2)$, while $I_{\mathrm{pas}}=O(N_{\max}/\Gamma^2)$. This is the signature of the critical enhancement. It is also clear that this enhancement emerges from the splitting of the real part of the Liouvillian eigenvalues for $\epsilon>\omega_0$, which allows λ_-^{-1} to be arbitrarily large for ϵ approaching ϵ_c, as $\lambda_-^{-1}=O(N_{\max}/\Gamma)$. As we will see in the next section, when considering *both* time and system size as a resource, the optimal scaling for the QFI is $O(N_{\max}t/\Gamma)$; see Eq. (5). CQS allows for the coherent use of time $t\sim\lambda_-^{-1}$, from which the quadratic scaling for the QFI follows. In the absence of the transient regime, i.e., for $\epsilon<\omega_0$, there is a single timescale for the dynamics given by $t\sim\Gamma^{-1}$, so the QFI scales linearly. This happens even if we initialize the system to a state other than vacuum, and, therefore, explains also why PQS shows a linear scaling for the QFI (see Fig. 2).

Relation to ultimate precision bounds—So far the analysis has been carried out considering $N_{\max}$ alone as a resource. In the occurrence of losses, it is not possible to use the entire time resource coherently. However, as QFI arises linearly with the number of repetitions and a shorter time of single realization allows for a bigger number of repetitions, for fair comparison, we should still treat both $N_{\max}$ and total time T as a resource. Then, to use them optimally, one should divide the total time T into smaller parts $t_{\mathrm{opt}}=\mathrm{argmax}_t I(t)/t$, and in total time T perform $M=T/t_{\mathrm{opt}}$ repetitions. For passive strategies, this leads to $MI_{\mathrm{pas}}\sim 2N_{\max}T/\Gamma$ for $N_{\max}\gg 1$, where t_{opt} decreases with increasing $N_{\max}$, see the Supplemental Material [63], Sec. V for details.

To analyze the critical protocol in this framework, note that, as in the transient regime the number of photons increases linearly with time for $\omega_0=\Gamma$, and close to the criticality the time of a single repetition scales roughly as $\lambda_-^{-1}\simeq 2N_{\max}/\Gamma$. Therefore, the number of repetitions decreases with $N_{\max}$ as $M\simeq T\Gamma/2N_{\max}$, so the scaling $I_{\mathrm{cr}}=O(N_{\max}^2/\Gamma^2)$ translates to $MI_{\mathrm{cr}}=O(N_{\max}T/\Gamma)$, as in passive strategy. It is also worth emphasizing that, to obtain the scaling $\propto N_{\max}T/\Gamma$ of the QFI, no quantum resources are needed, i.e., a protocol based on a coherent state with single repetition time $1/\Gamma$ and homodyne detection achieves this scaling as well.

Can this scaling be improved in any way? By applying results from [56,59], we show that the QFI for the estimation of the frequency of the cavity coupled to the thermal bath is fundamentally bounded by (see the Supplemental Material [63], Sec. VI):

$$I^{\mathrm{total}}_{\mathrm{cr,pas}}\leq\int_0^T\frac{2N(t)}{\Gamma(1+2n_B-\frac{n_B}{N(t)+1})}dt\lesssim\frac{2N_{\max}T}{\Gamma(1+2n_B)},\qquad(5)$$

where the second inequality holds for $N_{\max}/n_B\gg 1$. Here with the superscript "total" we stress the fact that the bound already includes the possibility of dividing the total time T into smaller parts and perform measurements between them (QFI scales linearly with the number of repetitions). While in this paper we discuss in detail the protocol based on phase transition in the occurrence of squeezing Hamiltonian, the above bound remains valid for any other metrological strategy, including all kinds of criticality, adaptiveness, partial measurements, etc. Note that, while optimal PQS saturates the bound in the limit of large $N_{\max}$, the CQS cannot perform as well, since the number of photons arises from 0. Therefore, after averaging, it needs to be strictly smaller than $N_{\max}$. Where, then, does the advantage of CQS manifest itself?

The ultimate bound (5) is derived by neglecting preparation and measurement time $t_{p,m}$. In many experiments, this is an unrealistic assumption. For instance, to initialize a linear resonator to a squeezed state with $N_{\max}$ photons, one

way involves pumping the resonator with a squeezed signal. Assuming the favorable situation that Γ represents the coupling with the preparation line, it then takes $O[\log(N_{\max})/\Gamma]$ time to prepare the cavity; see the Supplemental Material [63], Sec. VII. Discharging the resonator, essential to perform measurements on the output modes, requires the same time. Generally speaking, a more meaningful way to approach the problem is to divide T in $t_{\rm opt} = \mathrm{argmax}_t I(t)/(t + t_{p,m})$ parts. In Fig. 3, we show that, already for $t_{p,m} \simeq 2/\Gamma$, i.e., a time $1/\Gamma$ each for measuring and preparing the state, PQS performance is largely reduced while CQS performance remains virtually untouched. This is because in CQS the single-shot QFI achieves its maximum at a time much larger than Γ^{-1}, so $t_{p,m}$ is negligible. This leaves space for independent exploration by considering specific implementations of the protocols. For instance, preparation and measurement of the field *outside* the resonator can be further analyzed using the time-dependent input-output theory.

Finite-temperature dissipative case ($\Gamma > 0$, $n_B > 0$)—A similar analysis can be performed for arbitrary temperature. For the dynamics, we consider the critical system starting from a thermal state ρ_B with n_B photons and consider $\epsilon > \omega_0$. For the same values of ϵ, ω_0, the Liouvillian eigenvalues are unchanged, so the unitary and steady-state timescales are the same. Moreover, also ϵ_c and $I_{\rm cr}(t)$ are left unchanged. However, the mean number of photons at any time is $(1 + 2n_B)$ times bigger than in the zero-temperature case. It means that the same value of QFI would be obtained if the constraint for the number of photons would be also rescaled to $N'_{\max} = (1 + 2n_B)N_{\max}$. The same holds also for the passive strategy; see the Supplemental Material [63], Sec. VIII. Both protocols are therefore robust to thermal noise in the same way, in accordance to the bound (5).

Beyond the critical point—Lastly, we shall discuss whether it is possible to get an enhancement by exploiting the dynamics of a fast quench of the system, i.e., working at $\epsilon > \epsilon_c$, as proposed in Ref. [46]. For $\epsilon > \epsilon_c$, the number of photons grows exponentially in time, as $N(t) \sim e^{2\sqrt{\epsilon^2-\epsilon_c^2}t}/4$. Since the QFI is polynomial in the number of photons, also the QFI increases exponentially in time. One may then conclude that this strategy offers a great advantage. However, an analysis based on imposing a constraint on the number of photons in the resonator reveals that this strategy is suboptimal.

Consider for instance the noiseless case; see the Supplemental Material [63], Sec. III. Here, $I_{\rm cr}^{\epsilon>\epsilon_c}(t) \sim 4N^2(t)/(\epsilon^2 - \epsilon_c^2)$ for $t\sqrt{\epsilon^2 - \epsilon_c^2} \gg 1$. The optimal choice of ϵ, allowing for coherent use of all resources, under the photon number constraint $N(T) = N_{\max}$, is $\epsilon^2 \simeq \epsilon_c^2 + \log^2(4N_{\max})/4T^2$, which leads to $I_{\rm cr}^{\epsilon>\epsilon_c} = O(N_{\max}^2 T^2/\log^2 N_{\max})$. So, contrary to the case below the critical point, Heisenberg scaling with all resources is not possible at all.

Conclusions—We have compared passive quantum sensing strategies with protocols exploiting the dynamics of driven-dissipative critical systems. We have identified relevant frameworks in which critical quantum sensing outperforms passive quantum sensing for the parameter estimation task, in open quantum systems at arbitrary temperature. The considered minimal model describes the critical behavior of a broad class of systems, including finite-component phase transitions [21,26,64–66] and fully connected models [41–43]. PTs of this kind have been already observed with controllable atomic [64,70] and solid-state [65–68] quantum technologies. For critical models that do not belong to the considered class, such as many-body spin models, our Letter still provides a method to make a comparison with the ultimate precision performance. As the critical enhancement appears for dissipative systems and is robust against thermal noise and preparation and/or measurement time, our analysis paves the way for the development of *practical* critical quantum sensors in these experimental settings. Indeed, in some experimental contexts CQS sensing protocols can be even simpler to implement than standard sensing strategies, as the initialization does not depend on the prior, and the optimal measurement is a simple homodyne detection in all regimes.

Acknowledgments—We thank Rafał Demkowicz-Dobrzański and Pavel Sekatski for useful comments on fundamental bound on QFI. We acknowledge financial support from the Academy of Finland, Grants No. 353832 and No. 349199, from the U.S. DOE, National Quantum Information Science Research Centers, (SQMS) under Contract No. DE-AC02-07CH11359, from EU H2020 Quant ERA ERA-NET Cofund in Quantum Technologies QuICHE under Grant Agreements No. 731473 and No. 101017733, from the PNRR MUR Project No. PE0000023-NQSTI, from the National Research Centre for HPC, Big Data and Quantum Computing, PNRR MUR Project No. CN0000013-ICSC, and from PRIN2022 CUP 2022RATBS4.

[1] M. G. A. Paris, Quantum estimation for quantum technology, Int. J. Quantum. Inform. **07**, 125 (2009).
[2] C. L. Degen, F. Reinhard, and P. Cappellaro, Quantum sensing, Rev. Mod. Phys. **89**, 035002 (2017).
[3] P. Zanardi, M. G. A. Paris, and L. Campos Venuti, Quantum criticality as a resource for quantum estimation, Phys. Rev. A **78**, 042105 (2008).
[4] P. A. Ivanov and D. Porras, Adiabatic quantum metrology with strongly correlated quantum optical systems, Phys. Rev. A **88**, 023803 (2013).
[5] M. Bina, I. Amelio, and M. G. A. Paris, Dicke coupling by feasible local measurements at the superradiant quantum phase transition, Phys. Rev. E **93**, 052118 (2016).
[6] S. Fernández-Lorenzo and D. Porras, Quantum sensing close to a dissipative phase transition: Symmetry breaking

and criticality as metrological resources, Phys. Rev. A **96**, 013817 (2017).
[7] I. Frérot and T. Roscilde, Quantum critical metrology, Phys. Rev. Lett. **121**, 020402 (2018).
[8] P. A. Ivanov, Enhanced two-parameter phase-space-displacement estimation close to a dissipative phase transition, Phys. Rev. A **102**, 052611 (2020).
[9] C. Invernizzi, M. Korbman, L. Campos Venuti, and M. G. A. Paris, Optimal quantum estimation in spin systems at criticality, Phys. Rev. A **78**, 042106 (2008).
[10] S. S. Mirkhalaf, E. Witkowska, and L. Lepori, Supersensitive quantum sensor based on criticality in an antiferromagnetic spinor condensate, Phys. Rev. A **101**, 043609 (2020).
[11] A. Niezgoda and J. Chwedeńczuk, Many-body nonlocality as a resource for quantum-enhanced metrology, Phys. Rev. Lett. **126**, 210506 (2021).
[12] M. Tsang, Quantum transition-edge detectors, Phys. Rev. A **88**, 021801(R) (2013).
[13] K. Macieszczak, M. Guţă, I. Lesanovsky, and J. P. Garrahan, Dynamical phase transitions as a resource for quantum enhanced metrology, Phys. Rev. A **93**, 022103 (2016).
[14] A. Cabot, F. Carollo, and I. Lesanovsky, Continuous sensing and parameter estimation with the boundary time crystal, Phys. Rev. Lett. **132**, 050801 (2024).
[15] D.-S. Ding, Z.-K. Liu, B.-S. Shi, G.-C. Guo, K. Mølmer, and C. S. Adams, Enhanced metrology at the critical point of a many-body Rydberg atomic system, Nat. Phys. **18**, 1447 (2022).
[16] R. Liu, Y. Chen, M. Jiang, X. Yang, Z. Wu, Y. Li, H. Yuan, X. Peng, and J. Du, Experimental critical quantum metrology with the Heisenberg scaling, npj Quantum Inf. **7**, 170 (2021).
[17] M. M. Rams, P. Sierant, O. Dutta, P. Horodecki, and J. Zakrzewski, At the limits of criticality-based quantum metrology: Apparent super-Heisenberg scaling revisited, Phys. Rev. X **8**, 021022 (2018).
[18] V. Giovannetti, S. Lloyd, and L. Maccone, Advances in quantum metrology, Nat. Photonics **5**, 222 (2011).
[19] L. Garbe, M. Bina, A. Keller, M. G. A. Paris, and S. Felicetti, Critical quantum metrology with a finite-component quantum phase transition, Phys. Rev. Lett. **124**, 120504 (2020).
[20] S. Ashhab, Superradiance transition in a system with a single qubit and a single oscillator, Phys. Rev. A **87**, 013826 (2013).
[21] M.-J. Hwang, R. Puebla, and M. B. Plenio, Quantum phase transition and universal dynamics in the Rabi model, Phys. Rev. Lett. **115**, 180404 (2015).
[22] R. Puebla, M.-J. Hwang, J. Casanova, and M. B. Plenio, Probing the dynamics of a superradiant quantum phase transition with a single trapped ion, Phys. Rev. Lett. **118**, 073001 (2017).
[23] J. Peng, E. Rico, J. Zhong, E. Solano, and I. L. Egusquiza, Unified superradiant phase transitions, Phys. Rev. A **100**, 063820 (2019).
[24] H.-J. Zhu, K. Xu, G.-F. Zhang, and W.-M. Liu, Finite-component multicriticality at the superradiant quantum phase transition, Phys. Rev. Lett. **125**, 050402 (2020).
[25] N. Bartolo, F. Minganti, W. Casteels, and C. Ciuti, Exact steady state of a Kerr resonator with one- and two-photon driving and dissipation: Controllable Wigner-function multimodality and dissipative phase transitions, Phys. Rev. A **94**, 033841 (2016).
[26] S. Felicetti and A. Le Boité, Universal spectral features of ultrastrongly coupled systems, Phys. Rev. Lett. **124**, 040404 (2020).
[27] F. Minganti, L. Garbe, A. Le Boité, and S. Felicetti, Non-Gaussian superradiant transition via three-body ultrastrong coupling, Phys. Rev. A **107**, 013715 (2023).
[28] F. Minganti, V. Savona, and A. Biella, Dissipative phase transitions in n-photon driven quantum nonlinear resonators, Quantum **7**, 1170 (2023).
[29] T. L. Heugel, M. Biondi, O. Zilberberg, and R. Chitra, Quantum transducer using a parametric driven-dissipative phase transition, Phys. Rev. Lett. **123**, 173601 (2019).
[30] R. Di Candia, F. Minganti, K. V. Petrovnin, G. S. Paraoanu, and S. Felicetti, Critical parametric quantum sensing, npj Quantum Inf. **9**, 23 (2023).
[31] E. Rinaldi, R. Di Candia, S. Felicetti, and F. Minganti, Dispersive qubit readout with machine learning, arXiv:2112.05332.
[32] K. Petrovnin, J. Wang, M. Perelshtein, P. Hakonen, and G. S. Paraoanu, Microwave photon detection at parametric criticality, PRX Quantum **5**, 020342 (2024).
[33] T. Ilias, D. Yang, S. F. Huelga, and M. B. Plenio, Criticality-enhanced electric field gradient sensor with single trapped ions, npj Quantum Inf. **10**, 36 (2024).
[34] S.-W. Bin, X.-Y. Lü, T.-S. Yin, G.-L. Zhu, Q. Bin, and Y. Wu, Mass sensing by quantum criticality, Opt. Lett. **44**, 630 (2019).
[35] S.-B. Tang, H. Qin, B.-B. Liu, D.-Y. Wang, K. Cui, S.-L Su, L.-L. Yan, and G. Chen, Enhancement of quantum sensing in a cavity-optomechanical system around the quantum critical point, Phys. Rev. A **108**, 053514 (2023).
[36] Q.-K. Wan, H.-L. Shi, and X.-W. Guan, Quantum-enhanced metrology in cavity magnonics, Phys. Rev. B **109**, L041301 (2024).
[37] G. Mihailescu, A. Bayat, S. Campbell, and A. K. Mitchell, Multiparameter critical quantum metrology with impurity probes, arXiv:2311.16931.
[38] Z.-J. Ying, S. Felicetti, G. Liu, and D. Braak, Critical quantum metrology in the non-linear quantum Rabi model, Entropy **24**, 1015 (2022).
[39] D. Xie, C. Xu, and A. M. Wang, Quantum thermometry with a dissipative quantum Rabi system, Eur. Phys. J. Plus **137**, 1323 (2022).
[40] J.-H. Lü, W. Ning, X. Zhu, F. Wu, L.-T. Shen, Z.-B. Yang, and S.-B. Zheng, Critical quantum sensing based on the Jaynes-Cummings model with a squeezing drive, Phys. Rev. A **106**, 062616 (2022).
[41] L. Garbe, O. Abah, S. Felicetti, and P. Puebla, Critical quantum metrology with fully-connected models: From Heisenberg to Kibble–Zurek scaling, Quantum Sci. Technol. **7**, 035010 (2022).
[42] N. Lambert, C. Emary, and T. Brandes, Entanglement and the phase transition in single-mode superradiance, Phys. Rev. Lett. **92**, 073602 (2004).
[43] P. Ribeiro, J. Vidal, and R. Mosseri, Thermodynamical limit of the Lipkin-Meshkov-Glick model, Phys. Rev. Lett. **99**, 050402 (2007).

[44] M. Salado-Mejía, R. Román-Ancheyta, F. Soto-Eguibar, and H. M. Moya-Cessa, Spectroscopy and critical quantum thermometry in the ultrastrong coupling regime, Quantum Sci. Technol. **6**, 025010 (2021).
[45] Y. Chu, S. Zhang, B. Yu, and J. Cai, Dynamic framework for criticality-enhanced quantum sensing, Phys. Rev. Lett. **126**, 010502 (2021).
[46] K. Gietka, L. Ruks, and T. Busch, Understanding and improving critical metrology. Quenching superradiant light-matter systems beyond the critical point, Quantum **6**, 700 (2022).
[47] K. Gietka, Squeezing by critical speeding up: Applications in quantum metrology, Phys. Rev. A **105**, 042620 (2022).
[48] L. Garbe, O. Abah, S. Felicetti, and R. Puebla, Exponential time-scaling of estimation precision by reaching a quantum critical point, Phys. Rev. Res. **4**, 043061 (2022).
[49] C. Hotter, H. Ritsch, and K. Gietka, Combining critical and quantum metrology, Phys. Rev. Lett. **132**, 060801 (2024).
[50] V. Montenegro, U. Mishra, and A. Bayat, Global sensing and its impact for quantum many-body probes with criticality, Phys. Rev. Lett. **126**, 200501 (2021).
[51] R. Salvia, M. Mehboudi, and M. Perarnau-Llobet, Critical quantum metrology assisted by real-time feedback control, Phys. Rev. Lett. **130**, 240803 (2023).
[52] T. Ilias, D. Yang, S. F. Huelga, and M. B. Plenio, Criticality-enhanced quantum sensing via continuous measurement, PRX Quantum **3**, 010354 (2022).
[53] D. Yang, S. F. Huelga, and M. B. Plenio, Efficient information retrieval for sensing via continuous measurement, Phys. Rev. X **13**, 031012 (2023).
[54] G. Di Fresco, B. Spagnolo, D. Valenti, and A. Carollo, Multiparameter quantum critical metrology, SciPost Phys. **13**, 077 (2022).
[55] R. Demkowicz-Dobrzański and L. Maccone, Using entanglement against noise in quantum metrology, Phys. Rev. Lett. **113**, 250801 (2014).
[56] R. Demkowicz-Dobrzański, J. Czajkowski, and P. Sekatski, Adaptive quantum metrology under general Markovian noise, Phys. Rev. X **7**, 041009 (2017).
[57] S. Zhou and L. Jiang, Asymptotic theory of quantum channel estimation, PRX Quantum **2**, 010343 (2021).
[58] S. Kurdziałek, W. Górecki, F. Albarelli, and R. Demkowicz-Dobrzański, Using adaptiveness and causal superpositions against noise in quantum metrology, Phys. Rev. Lett. **131**, 090801 (2023).
[59] K. Wan and R. Lasenby, Bounds on adaptive quantum metrology under Markovian noise, Phys. Rev. Res. **4**, 033092 (2022).
[60] D. F. Walls and G. J. Wilburn, *Quantum Optics* (Springer, New York, 2008).
[61] A. Serafini, *Quantum Continuous Variables: A Primer of Theoretical Methods* (CRC Press, Boca Raton, 2017).
[62] G. Vallone, G. Cariolaro, and G. Pierobon, Means and covariances of photon numbers in multimode Gaussian states, Phys. Rev. A **99**, 023817 (2019).
[63] See Supplemental Material at http://link.aps.org/supplemental/10.1103/PhysRevLett.133.040801 for proofs and further details.
[64] M.-L. Cai, Z.-D. Liu, W.-D. Zhao, Y.-K. Wu, Q.-X. Mei, Y. Jiang, L. He, X. Zhang, Z.-C. Zhou, and L.-M. Duan, Observation of a quantum phase transition in the quantum Rabi model with a single trapped ion, Nat. Commun. **12**, 1126 (2021).
[65] G. Beaulieu, F. Minganti, S. Frasca, V. Savona, S. Felicetti, R. Di Candia, and P. Scarlino, Observation of first- and second-order dissipative phase transitions in a two-photon driven Kerr resonator, arXiv:2310.13636.
[66] Q.-M. Chen, M. Fischer, Y. Nojiri, M. Renger, E. Xie, M. Partanen, S. Pogorzalek, K. G. Fedorov, A. Marx, F. Deppe *et al.*, Quantum behavior of the Duffing oscillator at the dissipative phase transition, Nat. Commun. **14**, 2896 (2023).
[67] L. Zhong, E. P. Menzel, R. Di Candia, P. Eder, M. Ihmig, A. Baust, M. Haeberlein, E. Hoffmann, K. Inomata, T. Yamamoto *et al.*, Squeezing with a flux-driven Josephson parametric amplifier, New J. Phys. **15**, 125013 (2013).
[68] M. R. Vissers, R. P. Erickson, H.-S. Ku, L. Vale, X. Wu, G. C. Hilton, and D. P. Pappas, Low-noise kinetic inductance traveling-wave amplifier using three-wave mixing, Appl. Phys. Lett. **108**, 012601 (2016).
[69] We set α and r to be real, which is an optimal choice. This choice corresponds to squeezing the p quadrature and displacing along the x quadrature, as in Fig. 1.
[70] K. Baumann, C. Guerlin, F. Brennecke, and T. Esslinger, Dicke quantum phase transition with a superfluid gas in an optical cavity, Nature (London) **464**, 1301 (2010).